AJNR

Perfusion Imaging of Meningioma by Using Continuous Arterial Spin-Labeling: Comparison with Dynamic Susceptibility-Weighted Contrast-Enhanced MR Images and Histopathologic Features

H. Kimura, H. Takeuchi, Y. Koshimoto, H. Arishima, H. Uematsu, Y. Kawamura, T. Kubota and H. Itoh

AJNR Am J Neuroradiol 2006, 27 (1) 85-93
http://www.ajnr.org/content/27/1/85

ORIGINAL RESEARCH

Perfusion Imaging of Meningioma by Using Continuous Arterial Spin-Labeling: Comparison with Dynamic Susceptibility-Weighted Contrast-Enhanced MR Images and Histopathologic Features

H. Kimura
H. Takeuchi
Y. Koshimoto
H. Arishima
H. Uematsu
Y. Kawamura
T. Kubota
H. Itoh

PURPOSE: The goal of the present study was to determine the utility of continuous arterial spin labeling (CASL) for characterization of meningioma by MR perfusion imaging and to compare these results with those obtained from the T2 dynamic susceptibility contrast (T2DSC) method and from histopathologic examination.

METHODS: Twenty-one cases of meningiomas were examined at 1.5T. CASL perfusion imaging was implemented on the basis of multisection single-shot echo-planar imaging with velocity-driven adiabatic spin-inversion preparation. T2DSC perfusion imaging was also performed by using a double-echo spoiled gradient echo sequence in a section containing the tumor. By focusing on the regions of interest, maps of % signal intensity change and cerebral blood flow (CBF) were determined from CASL and cerebral blood volume (CBV). CBF and mean transit time (MTT) were obtained from T2DSC. The microvessel area (MVA) was determined from specimens immunostained with anti-CD31 in 14 cases by measuring the total amount of staining in each histologic section. Linear regression analysis was performed for rCBF values from both perfusion methods and for % signal intensity change and MVA.

RESULTS: There was a significant correlation between CBF values determined from both perfusion methods ($r^2 = 0.73$; $P < .001$); however, the slope from T2DSC to CASL was less than unity, likely because of the different vascular weighting used for each method. There was also a significant correlation between CASL-% signal intensity change and MVA determined by histopathology ($r^2 = 0.91$; $P < .00001$). Perfusion values were the greatest for angiomatous meningioma and lowest for fibrous meningioma when using either perfusion method.

CONCLUSIONS: CASL and T2DSC perfusion methods are comparable in the characterization of meningiomas. Further, CASL is of use in assessing tumor microcirculation.

The degree of angiogenesis is a key determinant of the malignant potential of a brain tumor. Although conventional MR imaging with gadolinium contrast is useful for the detection and structural characterization of brain tumors, enhancement after gadolinium reflects disruption of the blood brain barrier rather than a true assessment of tumor vascularity.

Recent advances in dynamic MR imaging have facilitated quantitative assessment of tumor microcirculation. For example, perfusion MR imaging typically uses T2 dynamic susceptibility contrast (T2DSC), which yields information regarding cerebral blood volume (CBV), cerebral blood flow (CBF), and mean transit time (MTT) from the time course of signal intensity change after contrast injection. Use of an appropriate input function also allows for absolute quantification based on the adequate tracer kinetic model.[1,2] As a result, T2DSC perfusion imaging has been used in the characterization of tumors,[3-5] acute strokes,[6,7] and dementia.[8,9] Despite these uses, the need for exogenous contrast agent is a significant limitation to the routine clinical use of this method.

Perfusion MR imaging can also be performed by using arterial spin-labeling (ASL) in which electromagnetically labeled arterial blood water is used as a freely diffusible intrinsic tracer for cerebral blood flow. Because of the constant exchange of water between tissue and capillary blood, continuous arterial spin labeling (CASL) alters the total magnetization in the tissue, which is dependent on the amount of perfusion. Subtraction of a control image without prior labeling produces a perfusion-weighted image. In clinical application, this technique has proved reliable and reproducible in the assessment of CBF in various disease states, including cerebrovascular disease,[10-12] degenerative disease,[13] and temporal lobe epilepsy.[14] There is, however, relatively little data regarding the use of ASL for characterization of human brain tumors,[15,16] thereby limiting its use in the clinical setting.

Thus, the goal of the present study was to determine the utility of CASL for characterization of meningioma by perfusion MR imaging and to compare these results with those obtained from the T2 dynamic susceptibility contrast (T2DSC) method and from histopathologic examination. Evaluation of patients with meningioma, which has a relatively homogenous histologic composition, was used to determine the utility of each type of perfusion signal intensity.

Received February 20, 2005; accepted after revision May 19.

From the Departments of Radiology (H.K., Y.Ko., H.U., Y.Ka., H.I.) and Neurosurgery (H.T., H.A., T.K.), Faculty of Medical Science, University of Fukui, Fukui, Japan.

Address correspondence to Hirohiko Kimura, MD, PhD, Department of Radiology, MRI, Faculty of Medical Science, University of Fukui, 23 Shimoaizuki, Yoshida-gun, Matsuoka-cho, Fukui 910-1193, Japan.

Materials and Methods

Patient Population. A total of 21 patients, 14 with histologically confirmed meningiomas and 8 with meningioma as demonstrated by the typical findings on conventional MR imaging, were studied. Informed consent was obtained from all patients.

Continuous Arterial Spin Labeling (CASL). Structural and perfusion imaging were performed on a SIGNA 1.5T unit (GE Medical Systems, Milwaukee, Wisc) by using a standard quadrature head coil. Conventional T1- and T2-weighted fast-spin-echo images were obtained in axial planes for structural imaging. The perfusion imaging was based on multisection single-shot spin-echo planar imaging with parameters of 64 × 64 imaging matrix, 22-cm field of view (FOV), 7-mm section thickness, 3-mm section gap, and 4100/21-millisecond TR/TE. Multisection image acquisition was performed without wait time between sections (7 sections each with 60-millisecond acquisition), resulting in a total acquisition time of 420 milliseconds. For the ASL of the perfusion imaging, the velocity-driven adiabatic spin-inversion method was employed. The radiofrequency (RF) pulse trains consisted of rectangular shapes of 98-millisecond duration that were applied continuously for 2.4 seconds with a duty cycle of 89% and a gradient strength of 0.3 Gauss/cm. An RF amplitude of 0.35 mG was used, which was based on the maximum inversion demonstrated in previous studies.[17] The label plane was located at the level of the pons/medulla junction to avoid the curvature of the petrous portion of the internal carotid artery (ICA) and to select the end portion of the ascending portion of the ICA, which typically runs straight in the inferior to superior direction. Sine wave (125 Hz) RF was used in control scans for the elimination of magnetization transfer effect under multisection acquisitions.[18] The label and control scans were temporally interleaved. Thirty pairs of tagged and control images were subtracted and summed on an off-line workstation. Perfusion signal intensity was normalized by local signal intensity on a pixel-by-pixel basis to allow comparisons between different examinations.

T2*-Weighted Dynamic Susceptibility Contrast-Enhanced MR Imaging (T2 DSC). First-pass bolus MR imaging was performed subsequent to the acquisition of CASL imaging. The section of the dynamic imaging was determined at the center of tumor level, which corresponded to the same section of one of 7 CASL perfusion images. To avoid the T1-shortening effect, the T1-effect was corrected by using a double echo-spoiled gradient echo (SPGR) sequence.[19] After the acquisition of conventional images and CASL, the contrast-enhanced dynamic studies were performed by using a pulse sequence as described elsewhere.[20] After 24 images were acquired for T1 measurements and precontrast baseline images, gadolinium diethylenetriamine penta-acetic acid (Gd-DTPA; 0.1 mmol/kg body weight) was rapidly injected via an intravenous route at a rate of 3 mL/s by using a MR imaging-compatible power injector (MR spectroscopy-50; Nemoto, Tokyo, Japan) followed by a 20-mL saline flush. During and after contrast injection, single-section double-echo SPGR sequence was run with the parameters of TR/TE1/TE2, 33.3/7/23; flip angle, 10°; NEX, 0.75; matrix size, 256 × 128; section thickness, 7 mm; and FOV, 22 × 16 cm. A set of approximately 50 images was obtained for dynamic studies with a temporal resolution and a total acquisition time of approximately 2.4 seconds and 3 minutes, respectively.

Histologic Specimens. All tumor specimens were routinely fixed with formalin and embedded in paraffin. In brief, sections were deparaffinized with xylene and alcohol, and immunohistochemical staining was performed by the labeled streptavidin biotin method. After endogenous peroxidase was deactivated with 3% H_2O_2 solution, sections were immunostained with anti-CD31 (DAKO, Botany, New South Wales, Australia) but not counterstained with hematoxylin. To quantify and evaluate the vascularity of the tumor, microvessel area (MVA) was determined by capturing digital images of the immunostained specimen at 200× magnification with a charge-coupled device color camera. MVA values were defined as a percentage of the total area in each field, respectively. The images were then analyzed with MAC Scope software (Mitani Co., Fukui, Japan) to measure the MVA by quantifying the total amount of staining in each section. Four fields were evaluated in each slide. The histologic analyses were performed by at least 2 observers (H.T. and H.A.) who were unaware of the results of the perfusion MR imaging techniques. Histologic comparison was conducted in 14 of 21 cases to determine whether there was any correlation with the perfusion parameters from the MR imaging methods.

Data Processing. All images were transferred to a personal computer workstation and analyzed by in-house software written by IDL (Research System, Boulder, Colo).

Quantification of Perfusion by Using CASL. ASL data were acquired by using a delayed acquisition method.[21] A modified 2-compartment model was used to describe the blood flow with intra- and extravascular water in perfect exchange under a continuously labeled condition. The perfusion (f) was calculated by using the following equation.[12,21]

$$1)\quad f = \exp\left(\frac{W}{T_{1app}}\right) * \exp\left(\delta\left(\frac{1}{T_{1a}} - \frac{1}{T_{1app}}\right)\right) * \frac{\lambda(M_b^{cntrl} - M_b^{tagg})}{2\alpha M_b^{cntrl} T_{1app}} \qquad (W \geq \delta)$$

where M_b is the equilibrium of tissue magnetization, $M_b^{cntrl:}$ is the equilibrium of tissue magnetization in control scan, M_b^{tagg} is the equilibrium of tissue magnetization in labeling scan, d is the tissue transit time from labeling to the tissue compartment of imaging plane, l is the brain/blood partition coefficient of water, a is the labeling efficiency of inversion pulse, W is the postlabel wait time, and T_{1app} is the longitudinal relaxation time of brain tissue with perfusion. The definition of T_{1app} is $(1/T1 + f/\lambda)^{-1}$, and $T1$ is brain tissue relaxation time without perfusion contribution. $T1_a$ is the $T1$ of arterial blood. Values of $\delta = 1200$ milliseconds, $\lambda = 0.9$ mL/g, $T1_a = 1.4$ seconds,[22] and $\alpha = 0.89$, which was the nominal duty cycle of the inversion pulse train, were assumed, and a 1.4-second postlabel wait time ($W = 1.4$ seconds) was used.

T2*DSC Perfusion. Dynamic susceptibility contrast MR images were analyzed by the deconvolution theory previously reported by Ostergaard et al[1] The T1-shortening effect (due to the leakage of contrast material into tumor tissue) was corrected by the dual-echo technique.[23] Measured signals of the first and second echo, $S_1(t)$ and $S_2(t)$, were converted to a relative concentration time curve, $\Delta R_2^*(t)$ on a pixel-by-pixel basis by using the following equation:

$$2)\qquad \Delta R_2^*(t) = -k\ln[s_2(t)/s_1(t)]/(TE2 - TE1) - R_{2,pre}^*$$

where TE1 and TE2 are the first and second echo time, and k is the coefficient of normalization from signal intensity change to contrast media concentration. The prebolus value $R_{2,pre}^*$ was obtained from the images before arrival of the contrast bolus. The arterial input function was tentatively determined in the same section of tumor (preferably larger vessels in plane, which was selected as 10 pixels with peak maximum $\Delta R_2^*(t)$ change). No calibration to absolute value was performed; however, the coefficient of k in Equation 2 was determined to correspond to a white matter blood flow of 22 mL/min/100 g.[2] Singular value deconvolution was performed on a pixel-by-pixel basis by using the arterial input function and the first pass concentration time curves. This process used a threshold of 0.05 to 0.15 for the singular values, depending on the data signal intensity–to-noise ratios.

Region of Interest Selection and Statistical Analysis. Tumors were included within region of interest in CASL-perfusion images

Table 1: Individual clinical information, conventional MRI, and histological subtypes of tumors

Patient No./ Age (y)/Sex	Location of Tumor	MRI findings on T2WI*	Histological subtype of Meningioma
1/82/F	Right frontal convex, en. plaque type	(++), Edema (+)	Atypical meningioma
2/58/F	Adjacent to the meninges of left Sylvian fissure	(+++)	Angiomatous/microcystic meningioma
3/67/F	Left sphenoid ridge	NA	Meningothelial meningioma
4/35/F	Suprasellar	(±)	Meningothelial meningioma
5/69/M	Frontal falx	(++), edema (+)	
6/49/M	Frontal fax	(++)	Fibrous type
7/78/M	Right frontal convex	(++)	Angiomatous meningioma
8/60/M	Parietal parasagittal	(++)	
9/60/F	Left cerebellar tentorial	(±)	Fibrous type
10/32/M	Right ventricle, trigonal region	(++)	
11/49/M	Right frontal convex	(±)	Atypical meningioma
12/79/M	Right frontal meninge, adjacent to Sylvian fissure	(±)	
13/50/F	Right cerebellar tentorial	(+)	Meningothelial meningioma
14/77/F	Left frontal falx	(+)	
15/53/F	Left parietal parasagittal	(+)	
16/55/F	Left sphenoid ridge	(++)	Meningothelial meningioma
17/38/M	Left parietal convex	(+), Edema (+)	Atypical meningioma
18/33/F	Left temporal fossa, cystic portion (+)	(++)	Meningothelial meningioma
19/76/F	Right temporal fossa	(±), Edema (+)	Clear cell meningioma
20/63/F	Right frontal parasagittal	(++)	
21/54/F	Right parietal convex	(++)	Meningothelial meningioma

*Signal intensity of meningioma is evaluated as high or low relative to cortical signal. The degree of hyperintensity in the tumor is divided into four groups: (±), (+), (++), and (+++) denote low to iso, iso to slightly high, high, and very high, respectively.

and T2* dynamic-perfusion images. Four typical regions of interest were selected by one of the authors (H.K.), who was aware of the diagnosis. These regions of interest consisted of mean tumor region, total section with tumor region, and normal-appearing gray matter and white matter. The averaged value of the total section, including the tumor region, was used for calculation of the tumor CBF ratio relative to the total section CBF. Five images of perfusion parameters were also sampled, including the absolute rCBF (CASL-rCBF) and percent signal intensity change (CASL perfusion weighed image: CASL-PWI) determined with the CASL method, and the rCBV, rCBF, and MTT, obtained from T2DSC perfusion images.

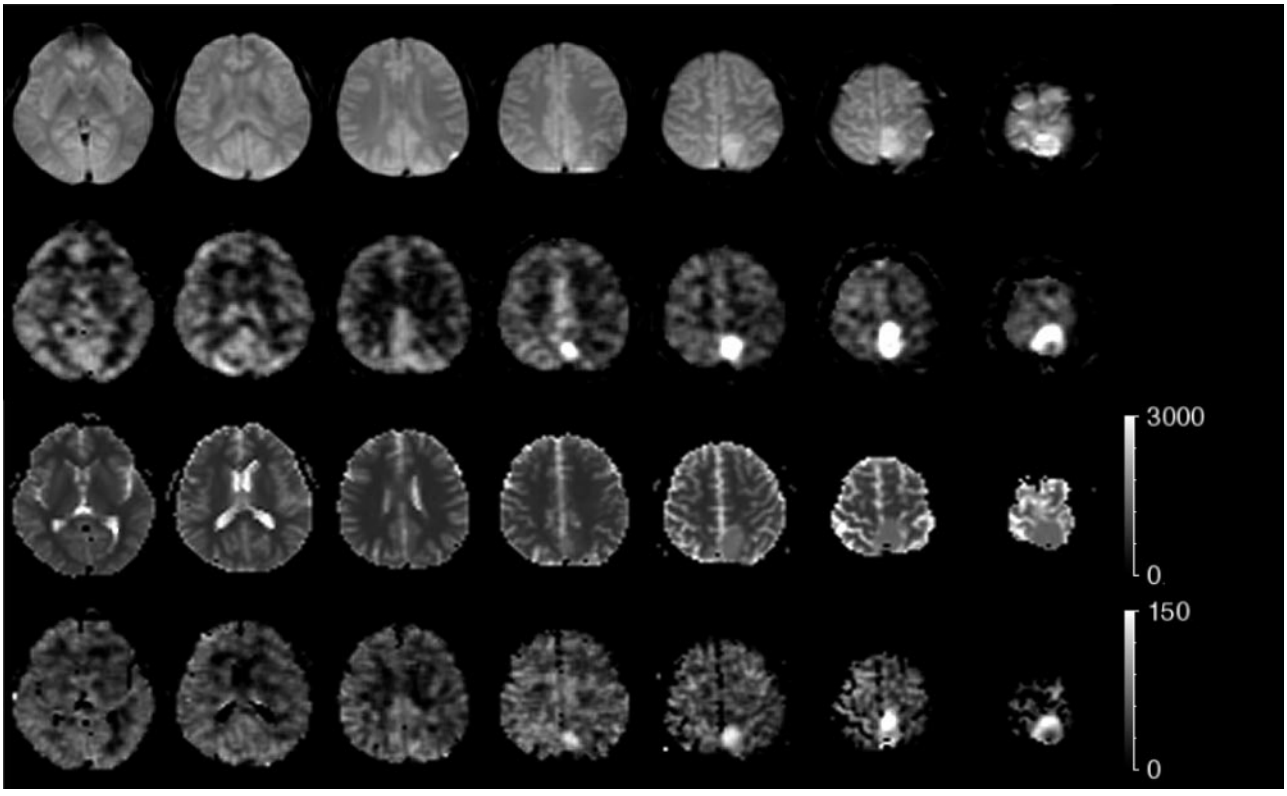

Fig 1. Multisection images obtained in a 60-year-old patient with meningioma (patient 8). Echo-planar images (4100/20 milliseconds), perfusion-weighted images, T1 maps, and quantitative CASL-rCBF maps are shown from the top to bottom rows. Values in rightmost column were expressed as milliseconds and mL/min/100 g in T1 maps and rCBF maps, respectively. The left parietal parasagittal meningioma is revealed as hyperperfusion in perfusion-weighted images and rCBF maps.

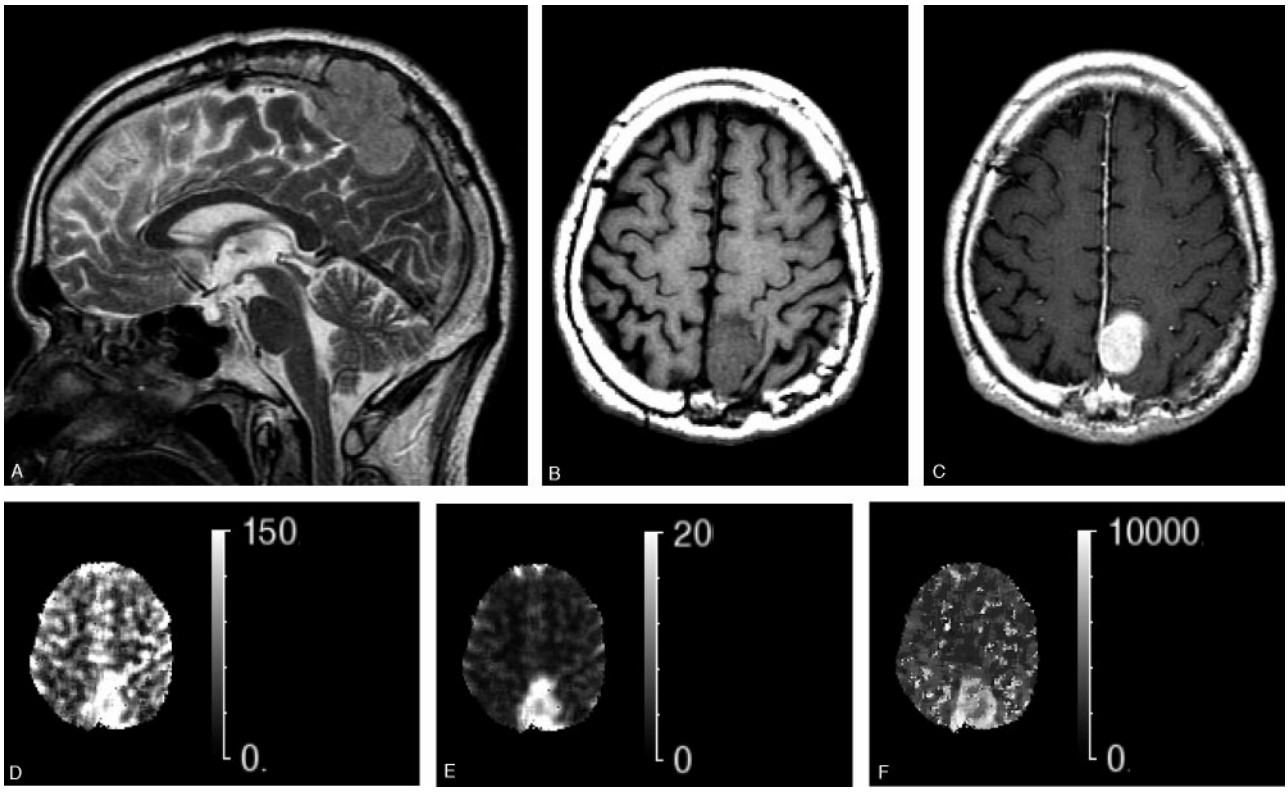

Fig 2. Conventional T2-weighted images and axial T1 images with and without Gd-DTPA. The perfusion maps obtained with T2DSC in a 60-year-old patient with parietal falx meningioma (patient 8, same as Fig 1). *A,* Sagittal T2-weighted image. *B,* T1-weighted image. *C,* Post-Gd-DTPA T1-weighted image. *D,* T2DSC perfusion image (rCBF map). *E,* T2DSC perfusion image (rCBV map. *F,* T2DSC perfusion image (MTT map). The tumor shows higher signal intensity than the cortex as well as enhancement on T2-weighted and post-Gd T1-weighted images. Dural tail sign is apparent in the anterior aspect of tumors. Note that the tumor protrudes into bone through the dura matter and cortical layers. The hyperperfusion signals are apparent on perfusion maps obtained with T2DSC, rCBF, and rCBV. Note that the MTT of tumor region has a slightly longer transit time relative to the parenchyma region.

Statistical analysis was performed by using Microsoft Excel (Microsoft, Redmond, Wash). Linear regression analysis was performed by using CASL-rCBF and T2DSC-rCBF in 19 patients in whom both perfusion images were successfully obtained (Table 2).

Results

Patient clinical information, meningioma description, and the results of T2-weighted spin-echo imaging are summarized in Table 1. Histologic examination of 14 specimens showed meningothelial ($n = 6$), fibrous ($n = 2$), angiomatous ($n = 2$), atypical ($n = 3$), and clear cell ($n = 1$) types.

Figure 1 shows a typical set of perfusion images performed by using the CASL method in a patient with meningioma, and Fig 2 shows the corresponding T2DSC perfusion images along with the conventional T1- and T2-weighted and post-Gd images.

Table 2 summarizes the measured CBF values in tumors and total section by using CASL and T2DSC methods. CBF was largest in the angiomatous meningiomas (Tables 1 and 2, patients 2 and 7), as demonstrated by a hyperintensity lesion on CASL and T2DSC CBF maps (Fig 3, patient 7). In contrast, CBF was lowest in the fibrous-type meningioma (Tables 1 and 2, patients 6 and 9), as demonstrated by a signal intensity with the same intensity as the neighboring cortical region on the CASL-rCBF map and a hyperintensity lesion on the T2DSC map (Fig 4, patient 6). The CASL-calculated CBF in the 6 meningothelial cases ranged from low to moderately high (Fig 5).

There was a significant correlation between CASL-rCBF and T2DSC-rCBF ($r^2 = 0.73$, $P < .001$), as demonstrated on the 2D plots in Fig 6. There was also a significant correlation between CASL and T2DSC in tumor rCBF/total-CBF ratios ($r^2 = 0.77$, $P < .001$), but the slopes of the correlation (0.47 and 0.74) were both less than unity in the value of CBF and the ratios relative to total blood flow, respectively (Fig 6).

Figure 7 displays a typical example of microvessel immunostaining by using CD31 and the extraction process of MVA on a histologic specimen from a patient with meningioma. There was a significant correlation between the signal intensity of meningiomas on CASL–% signal intensity change and MVA on histologic specimens ($r^2 = 0.91$, $P < .00001$), as demonstrated by the 2D plots in Fig 8, however, the correlation between CASL-rCBF and MVA was weaker ($r^2 = 0.61$, $P < .01$) than that between CASL–% signal intensity change and MVA. Data describing the correlation between MVA and other perfusion parameters are summarized in Table 3.

Discussion

The spin-tagging and T2DSC methods differ in terms of tracer characteristics. For example, CASL uses a diffusible tracer to yield measurements of CBF, whereas T2DSC uses intravascular nondiffusible contrast media to yield measurements of CBV. Previous studies suggest that characterization of cerebral perfusion by flow-sensitive alternative inversion recovery (FAIR) and T2DSC were comparable in normal patients and in patients with stroke.[24,25] This is consistent with results from the present study, which demonstrated compara-

Table 2: Measurements of perfusion values determined with CASL and T2DSC

Patient No.	CASL Perfusion			T2DSC Perfusion			
	Tumor CBF (mL/min/100 g)	Tumor (% Si)	Total CBF (mL/min/100 g)	Tumor CBV (mL/100 g)	Tumor CBF (mL/min/100 g)	Tumor MTT (s)	Total CBF (mL/min/100 g)
1	91	1.33	26	ND	ND	ND	ND
2	180	4.05	33	67	342	12	55
3	110	1.07	38	22	205	7	76
4	72	0.97	41	4	44	6	49
5	197	1.79	63	59	356	10	81
6	59	0.55	47	13	135	6	76
7	191	2.83	50	68	279	15	70
8	116	1.23	49	33	177	11	71
9	48	0.57	45	ND	ND	ND	ND
10	65	0.70	31	4	59	4	61
11	43	0.44	35	9	63	9	51
12	77	0.68	27	41	258	10	93
13	56	0.66	23	22	126	12	64
14	23	0.28	41	5	178	5	73
15	87	0.71	65	23	54	8	104
16	101	0.72	34	16	190	5	68
17	102	0.75	31	32	183	11	90
18	114	0.47	51	23	127	11	63
19	46	0.41	16	21	157	8	83
20	74	0.56	28	21	153	9	73
21	38	0.36	44	15	76	12	74

Note:—T2DSC indicates T2-dynamic susceptibility contrast; CASL, continuous arterial spin labeling; %SI, percentage signal change relative to local signal intensity; CBF, cerebral blood flow; CBV, cerebral blood volume; MTT, mean transit time.

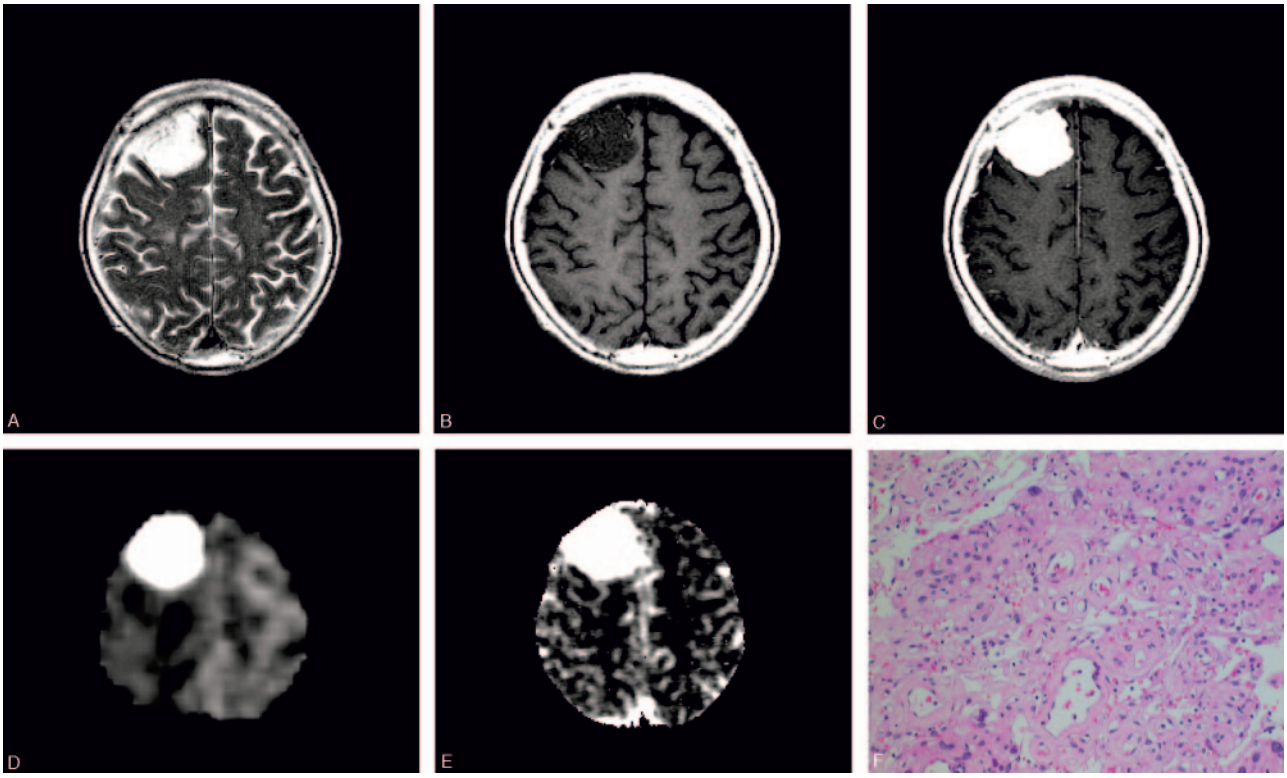

Fig 3. Axial conventional images and perfusion maps obtained with CASL and T2DSC in a 78-year-old patient with frontal convex meningioma (patient 7). *A,* T2-weighted image. *B,* T1-weighted image. *C,* Post-Gd T1-weighted image. *D,* CASL perfusion-weighted image (rCBF map). *E,* T2DSC perfusion image (rCBF map), The tumor shows a very high signal intensity and intense enhancement on T2-weighted and post-Gd T1-weighted images, respectively. The hyperperfusion signal intensity is apparent on perfusion maps obtained with CASL and T2DSC. *F,* HE-stained sections (×200) from the same case. The angiomatous subtype of meningioma was confirmed on histologic examination. The large thin-walled vessels in which red blood cells are contained are found throughout the specimen.

ble results in terms of meningioma CBF measurements when using either CASL or T2DSC.

Perfusion imaging is of use in the diagnosis and treatment of brain tumors. Indeed, previous studies have demonstrated that the T2DSC characterization of CBV could differentiate between low-grade and high-grade gliomas,[4,5,26] whereas oth-

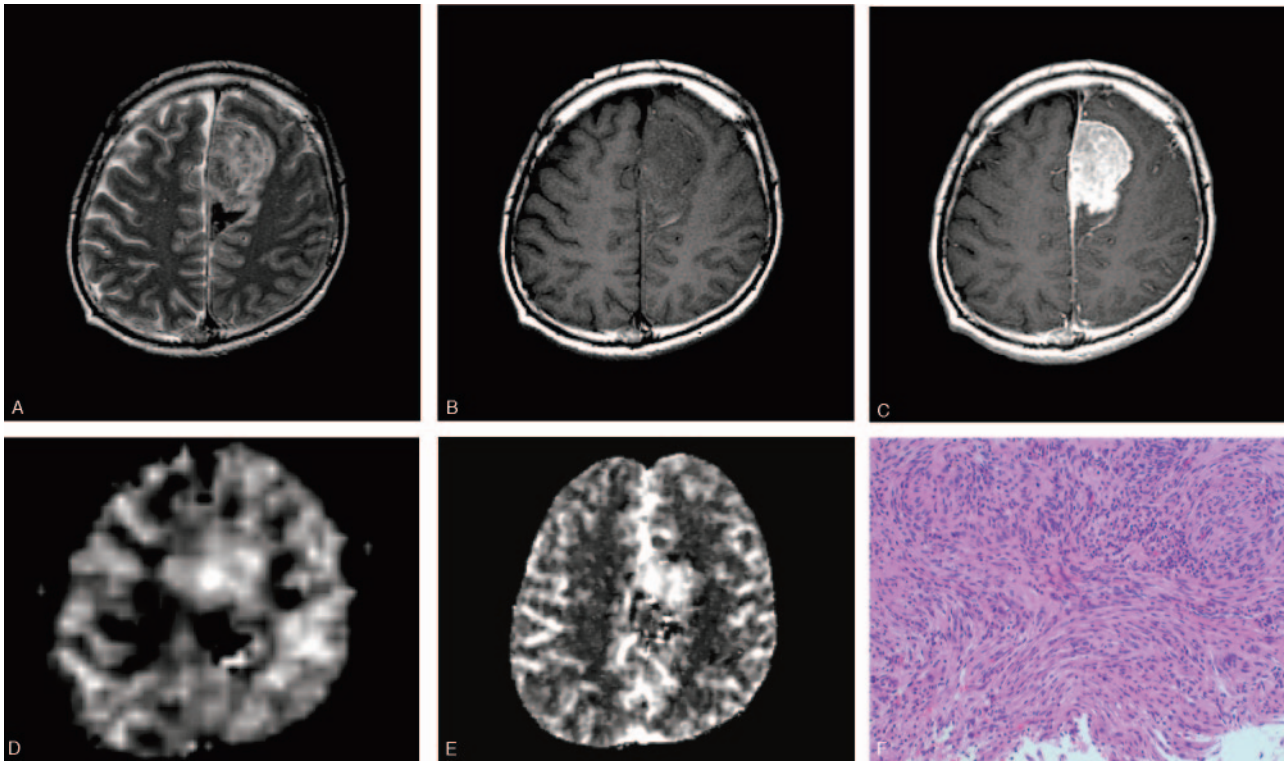

Fig 4. Axial conventional images and perfusion maps obtained with CASL and T2DSC in a 49-year-old patient with frontal falx meningioma (patient 6). *A,* T2-weighted image. *B,* T1-weighted image. *C,* Post-Gd T1-weighted image. *D,* CASL perfusion-weighted image (rCBF map). *E,* T2DSC perfusion image (rCBF map). The tumor shows slightly higher signal intensity than the cortex as well as good enhancement on T2-weighted and post-Gd T1-weighted-images, respectively. Note that the posterior aspect of tumor revealed very low signal intensity on T2-weighted images, corresponding to hemorrhagic change, which was also confirmed by CT imaging during the same period. The hyperperfusion signal intensity is apparent on perfusion maps obtained with CASL and T2DSC. *F,* HE-stained sections (×100) from the same case. The fibrous subtype of meningioma was confirmed on histologic examination. Microvessels are very scantly scattered in the specimen.

ers have reported that the response to irradiation therapy could be assessed by tumor perfusion.[27-29] The concordance of relative rCBF and the ratio relative to the averaged value of the whole section results when using either CASL or T2DSC (Fig 6) indicates that either technique could be used to assess tumor perfusion in patients with brain tumors. Although conventional MR imaging is adequate for characterization of the typical forms of meningioma, the technique may not be sufficient for full characterization of the more atypical forms of meningioma, such as with a large ventricle tumor or cystic component. In such cases, adjunctive modalities that describe perfusion parameters may be of particular utility, as meningioma is one of the most frequent hypervascular tumors that occur in the central nervous system. In fact, the present study demonstrated that the estimated values of CASL-rCBF were larger than the cortical CBF values in 18 of 21 cases (Table 2), provided the average total CBF value in gray matter is considered as 43 mL/min/100 g.[30] In particular, the CASL method was useful in differentiating the angiomatous subtype of meningioma from the other subtypes (Fig 5).

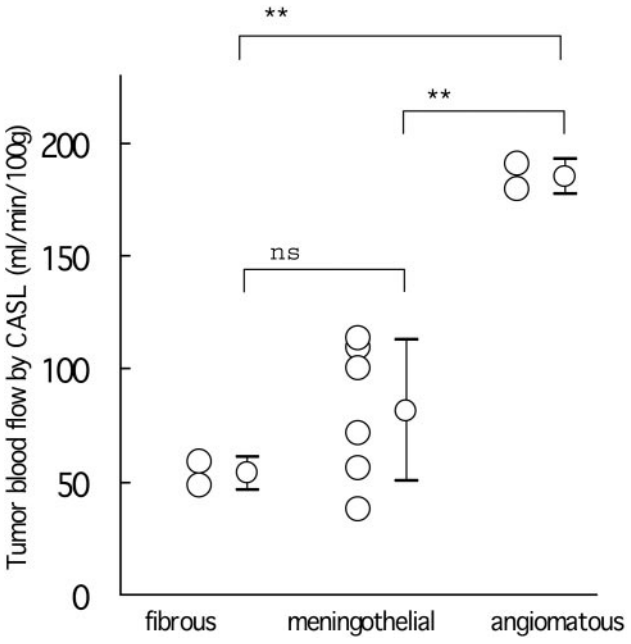

Fig 5. Tumor blood flow in each histologic group. The plot shows absolute tumor blood flow determined by continuous arterial spin-labeling in 10 patients with histologically proved meningiomas in each histologic subtype group. Three atypical and one clear cell subtype was excluded. Error bars indicate standard deviation. The result of Tukey-Kramer Multiple Comparisons Test is shown as ns (not significant: $P > .05$) and ** (significant difference: $P < .01$).

Determination of the arterial input function is required for the calculation of the absolute value of T2DSC-rCBF, MTT, and rCBV. Use of the single-section SPGR acquisition in the present study, however, made selection of a large-sized vessel for determination of the input function problematic. Thus, values were instead corrected to the white matter as a method of internal standardization. Alternatively, echo-planar imaging (EPI)–based T2DSC could have been used to overcome the limitation of single-section acquisition. However, this method would not eliminate the other problems associated with determination of the arterial input function. These prob-

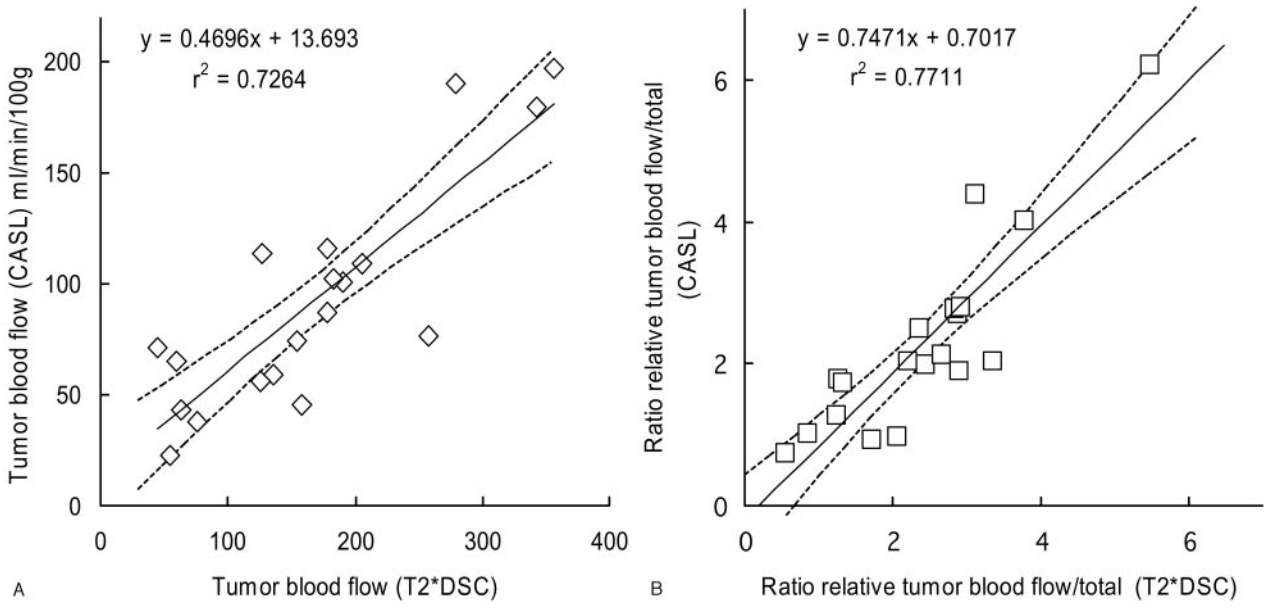

Fig 6. Scatter plots of tumor blood flow between T2DSC and CASL. *A,* CASL-rCBF versus T2DSC-rCBF. *B,* Ratio of tumor blood flow relative to whole section values between T2DSC and CASL. Linear regression analyses reveal high correlation in absolute rCBF values and relative ratios. The equation of the regression line is drawn in panels *A* and *B*. r^2 is the square value of correlation coefficient. Dashed lines indicate 95% confidence bands for the linear regression.

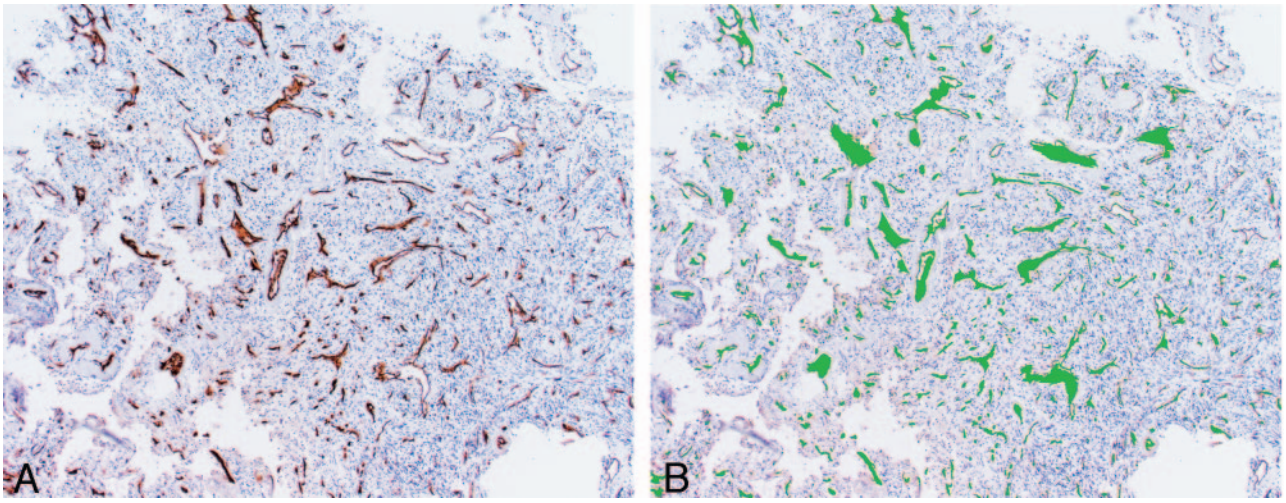

Fig 7. *A,* Microvessel immunostaining by using CD31 in meningioma (patient 6, same case as in Figs 1 and 2). The microvessel walls are positively stained. *B,* The microvessel areas are extracted automatically by the software. Note that the light green areas are overlaid on the immunostained specimen to the areas recognized as the lumen of microvessel structures.

lems include (1) artificially lowered CBF values due to the delay and dispersion of tracer bolus during passage from the large vessel to brain parenchyma, which cannot be corrected for without knowledge of the vascular network system[31]; (2) correction for contrast agent extravasation due to the permeability of tumor vessels, which may otherwise result in underestimation of relative CBV values[19]; and (3) the inability to separate the first pass from the contribution of extravasated contrast media when using double-echo SPGR sequences and a gamma variates function, which may result in obscuration of the bolus peak of $\Delta R_2^*(t)$ curve and lead to overestimation of the CBV value.

Arterial transit time is an important variable during CASL imaging. Because the effective time of labeling is limited, the perfusion-weighted signal intensity is inversely related to the transit time. This is problematic in that meningiomas may be supplied by an external carotid artery when the tumor is located in the convex region, meaning that labeling may be performed in both the internal carotid artery and the external carotid artery in the labeling plane. In fact, the present study characterized a large frontal convex meningioma as a homogenous hyperintensity lesion on CASL perfusion images, despite the redundant vascular contribution through the external carotid artery and internal carotid artery, which was confirmed by selective angiography in case 7 (Fig 3*D*).

Weighting of perfusion imaging performed with ASL is dependent on parameters of acquisition. In the case of CASL sequence, there is a shift in the perfusion image from large vessels toward the microvasculature and tissue signal intensity as the postdelay time increases, because most labeled spins may have enough time to diffuse into tissue. Other variables of vascular weighting include the type of echo and the crusher gradient used in the sequence. The spin-echo type of acquisition is considered to be more weighted in the microvasculature of perfusion than that obtained with gradient echo type of

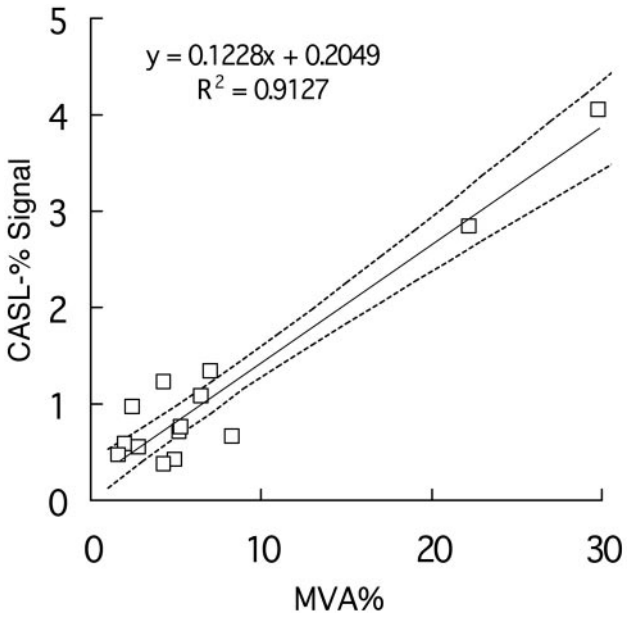

Fig 8. Microvessel area on histologic specimens (MVA) versus signal intensity change from CASL perfusion images in all 14 patients with meningioma. Linear regression analyses revealed high correlation, with an r^2 of 0.9127; 95% confidence bands are indicated by dashed lines. Regressed linear equation is shown as an inset in the graph.

acquisition.[32] Furthermore, the crusher gradient may eliminate the signal intensity from larger vessels.[33] Therefore, use of the spin-echo type with small crusher gradient and a 1.4-second postdelay time in the present study may have resulted in a perfusion signal intensity that was more weighted in the microvasculature and/or tissue.

Linear regression analysis showed a fairly good correlation between CASL and T2DSC for the ratio of tumor blood flow to mean blood flow, with an r^2 value of 0.77. The slope of correlation, however, was less than unity in the regression from T2DSC-rCBF to CASL-rCBF (Fig 6). A previous study reported a good correlation between ASL and T2DSC perfusion in brain tumors, with a slope of regression line of 1.04.[15] The reason for this discrepancy may be attributed to differences in the ASL sequence. For example, the previous report used a FAIR sequence, in which the acquisition timing is much more vascular weighted than that of CASL perfusion signal intensity.[21] Alternatively, the difference in blood flow condition between the 2 studies may result in underestimation of CASL-based blood flow calculations.[34] Indeed, the calculated blood flow of meningioma in this study was >100 mL/min/100 g, and tumor blood flow ratios from the present study were much larger than those from the previous study.[15] Finally, the intravascular nature of tracer in T2DSC technique may also result in overestimation of tumor blood flow and lower slope results.

The present study demonstrated a good correlation between the CASL-% signal intensity change and the MVA on histologic specimens (Fig 7), though 2 hypervascular cases may have produced a relatively large impact on the correlative significance due to the small number of cases studied. Because meningioma is more vascular than normal brain tissue, the labeled arterial spins in the tumor vasculature result in a hyperintensity on CASL-PWI; however, a longer MTT was a less likely cause of high signal intensity on CASL-PWI, because the coefficient of correlation between MVA and MTT, as determined by the T2DSC method, was relatively low ($r^2 = 0.29$, $P > .05$). By contrast, the correlation coefficient for MVA with either rCBV or rCBF, as obtained by T2DSC, was relatively high ($r^2 = 0.83$, $P < .0001$; $r^2 = 0.73$, $P < .001$). Therefore, the hyperintensity on CASL-PW (% signal intensity change) may be attributed to high CBV and high CBF, which is consistent with the strong correlation between CASL-% signal intensity change and MVA on histologic specimen. The hyperintensity on CASL-PWI may be a characteristic feature of meningiomas and may correspond to high blood flow and high vascularity.

Gd-DTPA is widely used in the clinical setting for the assessment of tumor perfusion. Although Gd-DTPA is safe, and perfusion SNR is high, the need for a rapid intravenous bolus (3–5 mL/s) remains the most significant limitation to use of T2DSC. By contrast, the advantages of ASL include its noninvasive nature, potential to yield absolute quantification,[21] ability to interrogate separate vascular territories,[35] and potential to achieve repeated measures.[36] Few institutions, however, use this technique routinely, primarily because of the lack of an available product pulse sequence. In fact, the most significant argument against using ASL is the lack of SNR. A previous study suggested that CASL may be of better utility than the pulsed ASL method when used in a higher magnetic field.[37] With the availability of more 3T magnets and the concomitant increase in T1 effect and perfusion SNR, the case for increased clinical implementation of ASL is more compelling.

Conclusions

The present study demonstrates that CBF measurements by CASL or T2DSC yielded comparable results in patients with meningioma and that these results are correlated with histopathologic assessment of vascularity. Further, CASL may be of use in distinguishing subtypes of meningioma. Differences in intrinsic contrast generation make CASL-rCBF values less dependent in the vascular bed, whereas T2DSC imaging can provide information regarding rCBV and MTT and is dependent on the definition of arterial input function. Absolute quantification of CASL-rCBF will require generation of an adequate compartment model to describe the exchange spins between arterial and tissue spins in the context of tumor tissue.

Table 3: Correlation of microvessel area and perfusion parameters

Perfusion Parameters	CASL: % Signal Change	CASL: rCBF	T2DSC: rCBV	T2DSC: rCBF	T2DSC: MTT
r^2	.91	.61	.83	.73	.29
Significance of correlation	$P < .00001$	$P < .001$	$P < .0001$	$P < .001$	$P < .05$

Note:—r^2: Squared Pearson's correlation coefficient. Significance of correlation; t test for simple linear regression was performed. The *p*-value is calculated using the t-distribution. CASL indicates continuous arterial spin labeling; T2DSC, T2-dynamic susceptibility contrast; rCBF, right cerebral blood flow; rCBV, right cerebral blood volume; MTT, mean transit time.

Acknowledgment

This work was supported by Grant-in-Aid for Scientific Research (A) (17209040) and by COE project from the Japan Society for the Promotion of Science.

References

1. Ostergaard L, Weisskoff RM, Chesler DA, et al. **High resolution measurement of cerebral blood flow using intravascular tracer bolus passages. Part I. Mathematical approach and statistical analysis.** *Magn Reson Med* 1996;36:715–25
2. Ostergaard L, Sorensen AG, Kwong KK, et al. **High resolution measurement of cerebral blood flow using intravascular tracer bolus passages. Part II. Experimental comparison and preliminary results.** *Magn Reson Med* 1996;36:726–36
3. Aronen HJ, Cohen MS, Belliveau JW, et al. **Ultrafast imaging of brain tumors.** *Top Magn Reson Imaging* 1993;5:14–24
4. Aronen HJ, Gazit IE, Louis DN, et al. **Cerebral blood volume maps of gliomas: comparison with tumor grade and histologic findings.** *Radiology* 1994;191:41–51
5. Knopp EA, Cha S, Johnson G, et al. **Glial neoplasms: dynamic contrast-enhanced T2*-weighted MR imaging.** *Radiology* 1999;211:791–98
6. Rother J, Guckel F, Neff W, et al. **Assessment of regional cerebral blood volume in acute human stroke by use of single-slice dynamic susceptibility contrast-enhanced magnetic resonance imaging.** *Stroke* 1996;27:1088–93
7. Ueda T, Yuh WT, Maley JE, et al. **Outcome of acute ischemic lesions evaluated by diffusion and perfusion MR imaging.** *AJNR Am J Neuroradiol* 1999;20:983–89
8. Bozzao A, Floris R, Baviera ME, et al. **Diffusion and perfusion MR imaging in cases of Alzheimer disease: correlations with cortical atrophy and lesion load.** *AJNR Am J Neuroradiol* 2001;22:1030–36
9. Harris GJ, Lewis RF, Satlin A, et al. **Dynamic susceptibility contrast MR imaging of regional cerebral blood volume in Alzheimer disease: a promising alternative to nuclear medicine.** *AJNR Am J Neuroradiol* 1998;19:1727–32
10. Chalela JA, Alsop DC, Gonzalez-Atavales JB, et al. **Magnetic resonance perfusion imaging in acute ischemic stroke using continuous arterial spin labeling.** *Stroke* 2000;31:680–87
11. Chalela JA, Kasner SE, McGarvey M, et al. **Continuous arterial spin labeling perfusion magnetic resonance imaging findings in postpartum vasculopathy.** *J Neuroimaging* 2001;11:444–46
12. Detre JA, Alsop DC, Vives LR, et al. **Noninvasive MRI evaluation of cerebral blood flow in cerebrovascular disease.** *Neurology* 1998;50:633–41
13. Alsop DC, Detre JA, Grossman M. **Assessment of cerebral blood flow in Alzheimer's disease by spin-labeled magnetic resonance imaging.** *Ann Neurol* 2000;47:93–100
14. Wolf RL, Alsop DC, Levy-Reis I, et al. **Detection of mesial temporal lobe hypoperfusion in patients with temporal lobe epilepsy by use of arterial spin labeled perfusion MR imaging.** *AJNR Am J Neuroradiol* 2001;22:1334–41
15. Warmuth C, Gunther M, Zimmer C. **Quantification of blood flow in brain tumors: comparison of arterial spin labeling and dynamic susceptibility-weighted contrast-enhanced MR imaging.** *Radiology* 2003;228:523–32
16. Gaa J, Warach S, Wen P, et al. **Noninvasive perfusion imaging of human brain tumors with EPISTAR.** *Eur Radiol* 1996;6:518–22
17. Maccotta L, Detre JA, Alsop DC. **The efficiency of adiabatic inversion for perfusion imaging by arterial spin labeling.** *NMR Biomed* 1997;10:216–21
18. Alsop DC, Detre JA. **Multisection cerebral blood flow MR imaging with continuous arterial spin labeling.** *Radiology* 1998;208:410–16
19. Uematsu H, Maeda M, Sadato N, et al. **Blood volume of gliomas determined by double-echo dynamic perfusion-weighted MR imaging: a preliminary study.** *AJNR Am J Neuroradiol* 2001;22:1915–19
20. Ishimori Y, Kimura H, Uematsu H, et al. **Dynamic T1 estimation of brain tumors using double-echo dynamic MR imaging.** *J Magn Reson Imaging* 2003;18:113–20
21. Alsop DC, Detre JA. **Reduced transit-time sensitivity in noninvasive magnetic resonance imaging of human cerebral blood flow.** *J Cereb Blood Flow Metab* 1996;16:1236–49
22. Barth M, Moser E. **Proton NMR relaxation times of human blood samples at 1.5 T and implications for functional MRI.** *Cell Mol Biol (Noisy-le-grand)* 1997;43:783–91
23. Miyati T, Banno T, Mase M, et al. **Dual dynamic contrast-enhanced MR imaging.** *J Magn Reson Imaging* 1997;7:230–35
24. Lia TQ, Guang CZ, Ostergaard L, et al. **Quantification of cerebral blood flow by bolus tracking and artery spin tagging methods.** *Magn Reson Imaging* 2000;18:503–12
25. Hunsche S, Sauner D, Schreiber WG, et al. **FAIR and dynamic susceptibility contrast-enhanced perfusion imaging in healthy subjects and stroke patients.** *J Magn Reson Imaging* 2002;16:137–46
26. Donahue KM, Krouwer HG, Rand SD, et al. **Utility of simultaneously acquired gradient-echo and spin-echo cerebral blood volume and morphology maps in brain tumor patients.** *Magn Reson Med* 2000;43:845–53
27. Fuss M, Wenz F, Scholdei R, et al. **Radiation-induced regional cerebral blood volume (rCBV) changes in normal brain and low-grade astrocytomas: quantification and time and dose-dependent occurrence.** *Int J Radiat Oncol Biol Phys* 2000;48:53–58
28. Fuss M, Wenz F, Essig M, et al. **Tumor angiogenesis of low-grade astrocytomas measured by dynamic susceptibility contrast-enhanced MRI (DSC-MRI) is predictive of local tumor control after radiation therapy.** *Int J Radiat Oncol Biol Phys* 2001;51:478–82
29. Weber MA, Thilmann C, Lichy MP, et al. **Assessment of irradiated brain metastases by means of arterial spin-labeling and dynamic susceptibility-weighted contrast-enhanced perfusion MRI: initial results.** *Invest Radiol* 2004;39:277–87
30. Yamaguchi T, Kanno I, Uemura K, et al. **Reduction in regional cerebral metabolic rate of oxygen during human aging.** *Stroke* 1986;17:1220–28
31. Calamante F, Gadian DG, Connelly A. **Delay and dispersion effects in dynamic susceptibility contrast MRI: simulations using singular value decomposition.** *Magn Reson Med* 2000;44:466–73
32. Fisel CR, Ackerman JL, Buxton RB, et al. **MR contrast due to microscopically heterogeneous magnetic susceptibility: numerical simulations and applications to cerebral physiology.** *Magn Reson Med* 1991;17:336–47
33. Ye FQ, Mattay VS, Jezzard P, et al. **Correction for vascular artifacts in cerebral blood flow values measured by using arterial spin tagging techniques.** *Magn Reson Med* 1997;37:226–35
34. Parkes LM, Tofts PS. **Improved accuracy of human cerebral blood perfusion measurements using arterial spin labeling: Accounting for capillary water permeability.** *Magn Reson Med* 2002;48:27–41
35. Werner R, Norris DG, Alfke K, et al. **Continuous artery-selective spin labeling (CASSL).** *Magn Reson Med* 2005;53:1006–12
36. Detre JA, Samuels OB, Alsop DC, et al. **Noninvasive magnetic resonance imaging evaluation of cerebral blood flow with acetazolamide challenge in patients with cerebrovascular stenosis.** *J Magn Reson Imaging* 1999;10:870–75
37. Wang J, Alsop DC, Li L, et al. **Comparison of quantitative perfusion imaging using arterial spin labeling at 1.5 and 4.0 Tesla.** *Magn Reson Med* 2002;48:242–54